catalysts

MDPI

Article

Metal-Doped HZSM-5 Zeolite Catalysts for Catalytic Cracking of Raw Bio-Oil: Exploring Activity toward Value-Added Products

María Eugenia Chiosso [1,2], Iratxe Crespo [3], Andrea Beatriz Merlo [4] and Beatriz Valle [3,*]

[1] Departamento de Ciencias Básicas y Experimentales, Universidad Nacional del Noroeste de la Provincia de Buenos Aires (UNNOBA), Junín 6000, Buenos Aires, Argentina; mechiosso@comunidad.unnoba.edu.ar
[2] Centro de Investigaciones y Transferencia del Noroeste de la Provincia de Buenos Aires (CITNOBA-UNNOBA UNSAdA-CONICET), Pergamino 2700, Buenos Aires, Argentina
[3] Department of Chemical Engineering, University of the Basque Country (UPV/EHU), P.O. Box 644, 48080 Bilbao, Biscay, Spain; iratxe.crespo@ehu.es
[4] Centro de Investigación y Desarrollo en Ciencias Aplicadas "Dr. Jorge J. Ronco" (CINDECA)—CCT-CONICET La Plata, Universidad Nacional de La Plata, Calle 47 No. 257, La Plata 1900, Buenos Aires, Argentina; andreamerlo@quimica.unlp.edu.ar
* Correspondence: beatriz.valle@ehu.es

Abstract: Catalytic cracking of bio-oil, conducted at atmospheric pressure without hydrogen supply, is a cost-effective and versatile approach for the targeted synthesis of biofuels and platform chemicals. The conversion of raw bio-oil follows intricate reaction pathways strongly influenced by the catalyst properties. In this work, we explore the use of various transition metals (Cr, Fe, and Zn) to modify the properties of HZSM-5 zeolite and assess their impact on the catalytic cracking of real raw bio-oil feedstock. The effect of metal loading on physical and chemical characteristics of metal-doped zeolite catalysts was studied through XRD, XRF, N_2 physisorption, NH_3-TPD, FTIR, H_2-TPR. The behavior of each catalyst was evaluated in a continuous two-step catalytic cracking system (TS-CC) operating at 450 °C and space-time 0.7 $g_{catalyst}h/g_{feed}$. The results highlight the importance of carefully selecting active metal species to optimize the performance of HZSM-5 in the catalytic cracking of bio-oil. Cr and Fe were found to be effective metals in increasing the selectivity of C_2–C_4 olefins in the gas product and mono-aromatics in the hydrocarbon liquid product, whereas the Zn-doped catalyst exhibits poor activity compared to bulk zeolite. Furthermore, a significant impact of the metal oxidation state on catalytic activity was observed, with reduced metals promoting the formation of H_2, CO, and CO_2 at the expense of hydrocarbon production.

Keywords: raw bio-oil; catalytic cracking; HZSM-5; active metal species; C_2–C_4 olefins; aromatics

Citation: Chiosso, M.E.; Crespo, I.; Merlo, A.B.; Valle, B. Metal-Doped HZSM-5 Zeolite Catalysts for Catalytic Cracking of Raw Bio-Oil: Exploring Activity toward Value-Added Products. *Catalysts* **2023**, *13*, 1198. https://doi.org/10.3390/catal13081198

Academic Editors: Junjian Xie and Qiang Deng

Received: 10 July 2023
Revised: 3 August 2023
Accepted: 9 August 2023
Published: 10 August 2023

1. Introduction

The transition toward a sustainable and low-carbon energy system requires innovative approaches for the efficient utilization of resources. In this context, the valorization of bio-oil produced through biomass pyrolysis has emerged as an appealing approach for decarbonizing the energy system. This is due to its renewable nature and carbon-neutral lifecycle. Bio-oil, with its complex oxygenated composition, offers a wide range of possibilities for obtaining value-added products. Among the various methods for converting bio-oil, catalytic cracking (CC) has emerged as a cost-effective and versatile approach for the targeted synthesis of biofuels and platform chemicals. This process is typically carried out at 400–500 °C, under atmospheric pressure, and without the need for hydrogen supply, which confers significant advantages in terms of costs and feasibility compared to the bio-oil hydrotreating process [1].

Nevertheless, the conversion of bio-oil oxygenates is a highly intricate process involving multiple reaction pathways, including deoxygenation (decarboxylation, decarbonyla-

tion, dehydration), C–C bond cleavage, oligomerization/cracking, alkylation, isomerization, and hydrogen-transfer reactions. The properties of the catalyst used strongly influence the prevalence of these reaction pathways.

Zeolites, particularly those with MFI morphology such as HZSM-5, have been widely employed in the conversion of biomass pyrolysis vapors and bio-oil into hydrocarbons [2,3]. The appropriate balance between acid strength and shape selectivity of ZSM-5 is considered crucial for its high selectivity toward aromatic hydrocarbons, including BTXE (benzene, toluene, xylenes, and ethylbenzene) [4,5]. These monoaromatics are in high demand as they serve as basic chemicals for the production of value-added products, such as plastics, fibers, pesticides, and fuel blending additives. Although HZSM-5 is considered an efficient catalyst for the bio-oil upgrading, its performance is usually improved by incorporation of metals within the zeolite framework to modify its acid properties and activity for reactions such as cracking, dehydration, aromatization, and oligomerization. Modification of HZSM-5 acidity by metal loading is an effective approach for achieving the desired upgrading results and enhancing coking resistance [6,7].

Doping metals on HZSM-5 zeolite can be achieved through two main methods: impregnation and ion exchange. In the impregnation method, metals are incorporated by depositing metal species onto the zeolite structure, whereas ion exchange involves the substitution of Si or Al ions with metal ions in the zeolite. The choice between these methods depends on the specific requirements of the catalytic application. Ion exchange provides controlled metal loading and a uniform distribution with stronger metal-support interaction, but it is primarily suitable for cationic metals, which may limit the range of metal species that can be incorporated. The catalyst synthesis also involves a more time-consuming and complex process, requiring careful control of pH, temperature, and concentration. On the other hand, impregnation with solutions of metal salts is favored for its simplicity and economic advantages, making it the most frequently applied method to introduce transition metals into zeolite crystals [6,8]. In this study, we focused on the incipient wetness impregnation method to incorporate metal species into ZSM-5 zeolite due to the flexibility of the process, which allows the incorporation of various metal species at relatively high metal loadings. Additionally, impregnation is a straightforward and easy-to-scale-up process, making it suitable for industrial applications.

Transition metal modification has been widely reported as an effective way for the improvement of HZSM-5 catalyst performance for biomass and bio-oil upgrading. However, careful consideration should be given to the selection of metal species and doping amounts. In this study, we focus on comparing the activity of HZSM-5 zeolite doped with chromium (Cr), iron (Fe), and zinc (Zn) for the catalytic cracking of raw bio-oil feedstock. The selection of these metals is driven by their relatively abundant and cost-effective nature when compared to metals such as Ni and Co, which although effective for the production of aromatics [9,10], are more expensive and less readily available. Additionally, Fe, Cr, and Zn are known for their good thermal stability and resistance to deactivation under harsh reaction conditions typically encountered in bio-oil cracking [11]. Obviously, their presence as modifiers can also influence the selectivity of the bio-oil catalytic cracking process, promoting the formation of specific valuable products.

Fe-modified ZSM-5, in particular, has demonstrated improved catalytic selectivity toward monoaromatic hydrocarbons (MAHs) in catalytic fast pyrolysis of biomass processes. These catalysts exhibited enhanced deoxygenation activity and higher BTX selectivity compared to the parent ZSM-5, attributed to the creation of new active sites and inhibition of repolymerization [12,13]. Mohiuddin et al. [14] studied the modification of ZSM-5 by impregnation of different loadings (0.5–5 wt%) of Fe and Cr in order to enhance the catalytic cracking of refinery naphtha to produce light olefins. According to their results, Fe acted as a promoter of olefins selectivity, in particular propylene, with the best value achieved for Fe loading of 2 wt%. Modification with Cr caused a decrease in selectivity to light olefins and an increase in BTX selectivity, with the highest value obtained with 2% Cr-ZSM-5 catalyst. Modification of HZSM-5 with 2 wt% of Zn was reported to increase the content of strong

acid sites, resulting in higher BTX (benzene, toluene, and xylene) yields during bio-oil upgrading. However, excessive Zn doping (10 wt%) was stated to decrease acidity and physical characteristics, negatively impacting reactant and product diffusion within the zeolite pores and reducing BTX yield [15].

In this work, various characterization techniques, including N_2 physisorption, X-ray diffraction (XRD), X-ray fluorescence (XRF), H_2-temperature programmed reduction (H_2-TPR), ammonia temperature programmed desorption (NH_3-TPD), and Fourier-transform infrared spectroscopy (FTIR) were employed to analyze the textural properties, acidity, and reducibility of the metal-doped HZSM-5 catalysts. Catalytic behavior was evaluated in a continuous two-step catalytic cracking system (TS-CC) operating at atmospheric pressure. Furthermore, the impact of the oxidation state (reducibility) of the metal species on the conversion of oxygenates and selectivity toward hydrocarbon products was investigated given that the oxidation state of the metal dopants can significantly influence catalytic activity and selectivity [16].

The main contribution of this paper is that the comparative study of metal-doped HZSM-5 catalysts was conducted for the valorization of raw bio-oil. Due to the bio-oil complexity, this area of research has received limited attention in the literature, which primarily focuses on the catalytic pyrolysis of biomass and catalytic cracking of model oxygenated compounds. The feedstock used in this study consists of 80 wt% actual raw bio-oil and 20 wt% methanol, which is necessary for stabilizing real bio-oils during storage. Therefore, the findings of this study have direct applicability to the scaling-up of the process.

Consequently, the findings from this study are significant for advancing the industrial implementation of bio-oil valorization. They contribute to a better understanding of the role of metal dopants in the catalyst activity for the selective production of hydrocarbons and/or oxygenates of primary interest, such as fuels or raw materials. By investigating the impact of various transition metals on the performance of HZSM-5 zeolite, this study sheds light on the selection of optimal active metal species for the development of highly active and selective catalysts.

2. Results and Discussion

2.1. Physicochemical Properties of Catalysts

The textural properties (specific surface area, micropore volume, and mesopore volume) of the bulk HZSM-5 zeolite catalyst (Bulk HZ-30) and each metal-doped catalyst (Cr-Z30, Fe-Z30, and Zn-Z30) are compared in Table 1. The results show that the BET surface area of the chromium-doped catalyst (Cr-Z30) hardly varies compared to the bulk zeolite, whereas in the case of iron (Fe-Z30) and zinc (Zn-Z30) a slight decrease (around 20 $m^2\ g^{-1}$) can be noticed. These results are attributed to the slight decrease in micropore volume. The values of mesopore volume, provided by the alumina matrix used for preparing the catalysts (described in Section 3.1) hardly varies. This fact confirms that the alumina matrix provides a similar mesoporous structure in all the catalysts.

Table 1. Textural properties and acidity of bulk HZSM-5 catalyst and metal-doped catalysts.

	Bulk HZ-30	**Cr-Z30**	**Fe-Z30**	**Zn-Z30**
S_{BET} ($m^2\ g^{-1}$)	267	271	254	251
$V_{Micropore}$ ($cm^3\ g^{-1}$)	0.06	0.06	0.05	0.04
$V_{Mesopore}$ ($cm^3\ g^{-1}$)	0.31	0.29	0.29	0.30
Acidity ($\mu mol_{NH3}\ g^{-1}$)	227	170	175	128

The values of total acidity quantified by NH_3-TPD reveal a lower acidity of the metal-doped catalysts compared to the bulk Z30 catalyst (Table 1), especially in the case of the zeolite doped with Zn (Zn-Z30). The nature of the acid sites (Brønsted and Lewis) was analyzed by FTIR of adsorbed pyridine and results are depicted in Figure 1.

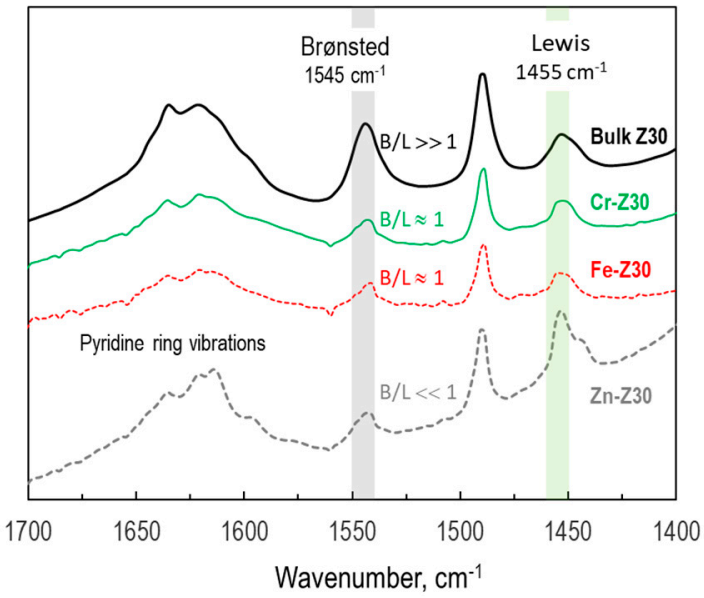

Figure 1. FTIR spectra of bulk HZSM-5 catalyst and metal-doped catalysts after saturation with pyridine.

All the FTIR spectra (Figure 1) reveal a clear band at 1545 cm^{-1}, which is associated with pyridinium cations ($PyrH^+$) formed by pyridine protonation on Brönsted acid sites, and the band at 1455 cm^{-1}, which is related to pyridine adsorbed on Lewis acid sites. The peak group observed at 1580–1660 cm^{-1} corresponds to ring vibrations of pyridine molecules. The density of Brönsted and Lewis acid sites is proportional to the intensity of these bands, considering the Emeis molar extinction coefficients [17].

The acidity characterization confirms that the introduction of Cr, Fe, and Zn as metal cations into the framework of HZSM-5 reduces the number of available strong Brønsted acid sites and creates new Lewis acid sites. This effect was clearly evidenced by the decrease in the Brønsted/Lewis ratio (B/L) observed in Figure 1, which is particularly pronounced in the case of Zn-Z30. These results are consistent with the decrease in the overall acidity of the metal-doped catalysts, as shown in Table 1.

The results of XRF measurements of metal-doped catalysts confirmed that metal loading was close to nominal contents, with 0.73 wt% in Zn-Z30, 0.94 wt% in Cr-Z30, and 1.08 wt% in Fe-Z30. The major metallic species identified in each catalyst were ZnO, Cr_2O_3, and Fe_2O_3, respectively.

In Figure 2a, the H_2-TPR results for the metal-doped zeolites are shown. This technique provides valuable insights into the reducibility and redox properties of the incorporated metal species. The TPR profile of Fe-Z30 catalyst shows a distinct reduction peak at 345 °C, followed by two broader zones with maxima at 450 and 540 °C, indicating the presence of different iron oxide species. The low-temperature peak is commonly attributed to the reduction of easily reducible iron oxide species (Fe_2O_3 to Fe_3O_4), the middle-temperature peak is associated to the reduction of Fe_3O_4 to FeO, and the high-temperature peak corresponds to the reduction to metallic Fe species with higher stability [18,19].

The TPR profile of the Cr-Z30 catalyst exhibits two reduction zones, with a first peak at 340 ºC and a broader reduction zone in the 400–600 °C range. In general, the first peak could be attributed to the reduction of chromium species in high oxidation states to Cr(III), while the second corresponds to the reduction of Cr(III) to Cr(II) species [20]. Recent studies also suggest the existence of Cr(III) in two distinctive environments, with Cr_2O_3 present either as crystallites or as grafted species (less reducible) [21].

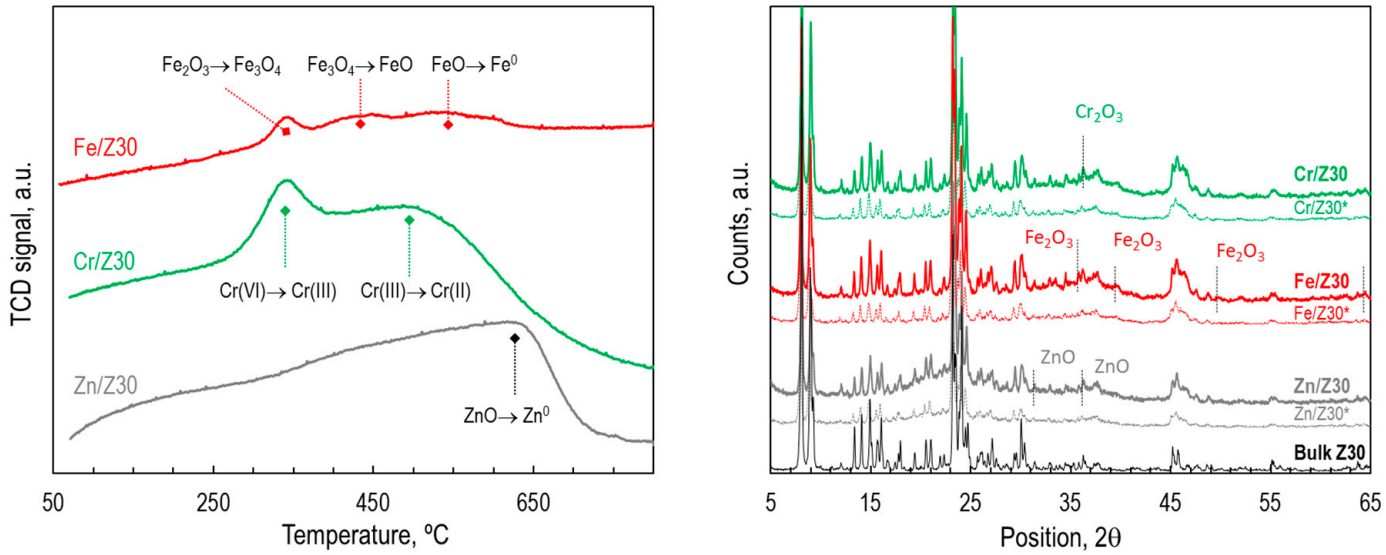

Figure 2. (**a**) H_2-TPR profiles of metal-doped catalysts; (**b**) XRD patterns of bulk Z30 and metal-doped catalysts before and after reduction (*) at 450 °C for 2 h under 10 mL min^{-1} H_2/N_2 flow.

The TPR results of the Zn-Z30 catalyst show an increasing profile with a virtual maximum at ca. 650 °C. These findings are consistent with those reported by other authors revealing the low reducibility of ZnO under usual conditions. Wan et al. [22] concluded that the reduction of ZnO barely reaches completion, even after subjecting it to harsh treatment with H_2 for 4 h at 650 °C.

Figure 2b depicts the XRD profiles of the bulk zeolite Z30, the fresh samples of metal-doped catalysts, and reduced samples (marked with an asterisk *) after in situ reduction at 450 °C for 2 h under 10 mL min^{-1} H_2/N_2 flow. The Bulk Z30 pattern exhibits peaks corresponding to crystalline ZSM-5 zeolite, with more intense peaks in the 7–9° and 22–25° ranges. Although metal-doped samples show slightly less defined peaks compared to the bulk zeolite, no significant changes in crystallinity are induced by the impregnation with Cr, Fe, or Zn. These results, along with the slight change detected in BET surface areas (Table 1), suggest good dispersion of metal species within the zeolite structure.

In the Fe-Z30 sample, several peaks corresponding to Fe_2O_3 could be detected, despite XRD peaks of metal oxides can be usually overlapped by those of HZSM-5, especially for low metal contents [23]. In the Cr-Z30 sample, XRD analysis detected only peaks attributed to Cr_2O_3 (Figure 2b). The peaks corresponding to CrO_3 phase were masked by the HZSM-5 peaks. It is worth noting that in this catalyst both CrO_3 and Cr_2O_3 phases can coexist, representing Cr(VI) and Cr(III), respectively. The presence of both chromium oxide phases was confirmed by the H_2-TPR results (Figure 2a). Our results are consistent with those reported by Mohiuddin et al. [14] and de Oliveira et al. [24] for Fe and Cr impregnated ZSM-5 in the 2.5–5 wt% range.

Upon reduction, a slight decrease in peak intensity was observed compared to fresh catalysts. In none of the reduced catalyst samples were signals of the metals observed because the metal loading was too low or the metal crystallites were too small for X-ray diffraction, indicating a high dispersion into the zeolite structures.

2.2. Evaluation of Activity for Catalytic Cracking of Bio-Oil

The behavior of bulk zeolite and metal-doped catalysts was evaluated in terms of reactants conversion (bio-oil oxygenates and methanol in the feed), product yields (CH_4, C_2–C_4, CO, CO_2, C_{5+} hydrocarbons, and water produced), and selectivity to hydrocarbons of interest, i.e., C_2–C_4 olefins and monoaromatics (BTXE and alkylbenzenes). These parameters were quantified according to Equations (1)–(4), defined in Section 3.5. The catalytic

cracking experiments were conducted at 450 °C; with a space-time of 0.7 $g_{catalyst}$ $h(g_{feed})^{-1}$ and time on stream of 0.5 h. With the aim of simplifying the presentation of the results to allow a clear and direct comparison of the catalysts' performance, the results correspond to the overall values of conversion and yields obtained throughout each reaction.

In Figure 3, the results of conversion (both of bio-oil oxygenates and methanol contained in the feed) using the bulk zeolite catalyst (Bulk Z30) are compared with those obtained with the different metal catalysts. This figure also displays the yields of products in the gaseous stream (C_2–C_4, CO, CO_2, CH_4, and dimethyl ether), as well as the selectivity to light olefins (C_2–$C_4^=$) achieved with each catalyst.

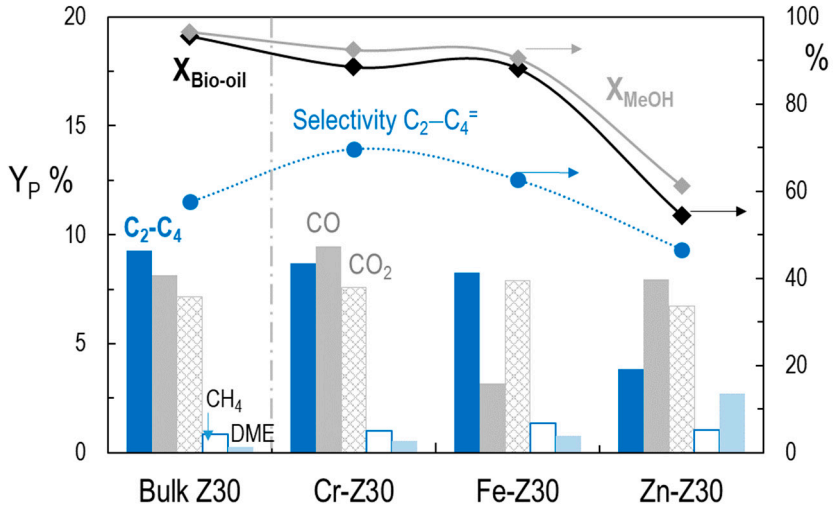

Figure 3. Comparison of oxygenates conversion (%), gaseous product yields (Y_P) and selectivity toward light C_2–C_4 olefins (%) obtained with bulk HZSM5 catalyst and metal-doped catalysts.

Figure 4 shows the yields of C_{5+} hydrocarbons obtained in the liquid product, which were categorized into BTXE (benzene, toluene, xylenes, ethylbenzene), C_5–C_{12} hydrocarbons (alkylbenzenes, naphthalenes, and aliphatics), and C_{12+} polyaromatics (PAHs). Additionally, the selectivity to mono-aromatic hydrocarbons (MAH = BTXE + alkylbenzenes) achieved with each catalyst is presented.

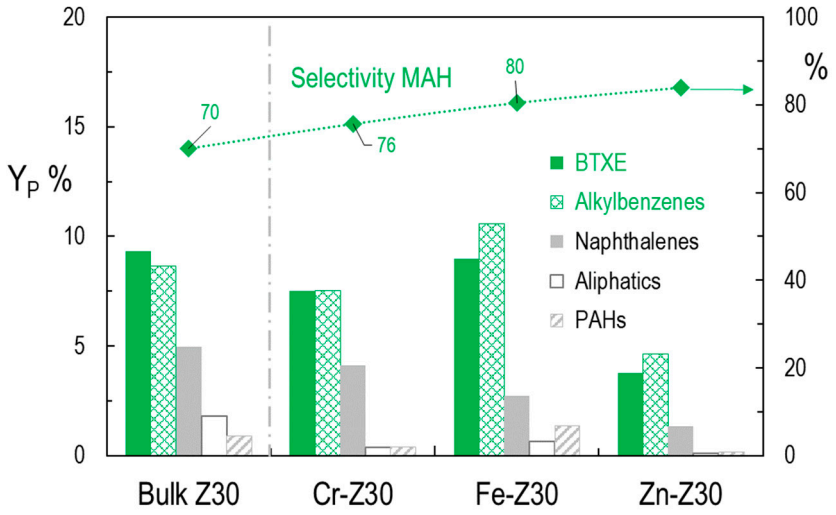

Figure 4. Comparison of liquid product yields (Y_P) and selectivity toward monoaromatic hydrocarbons (MAH) obtained with bulk HZSM-5 catalyst and metal-doped catalysts.

The results reveal that the addition of metals has an impact on the catalytic behavior of HZSM-5, altering its activity and selectivity. The results demonstrate that the zinc-doped zeolite (Zn-Z30) exhibits poor activity, with considerably lower bio-oil conversion (54%) compared to bulk zeolite (96%). On the other hand, the chromium and iron-doped zeolites show only slightly lower conversion, with values above 86% (Cr-Z30) and 88% (Fe-Z30) (Figure 3).

Furthermore, it is observed that the addition of metal causes changes in the product distribution, resulting in reduced yields of light hydrocarbons C_2–C_4 in all cases, although a higher selectivity toward light olefins was observed, except for Zn-Z30 (Figure 3).

Regarding the yield of C_{5+} liquid hydrocarbons (Figure 4), the addition of metals leads to a slight increase in the selectivity toward monoaromatic hydrocarbons (MAH). Notably, there are significant differences in the yield of these products depending on the metal used. While Cr-Z30 and Zn-Z30 exhibit lower yields, the Fe-Z30 catalyst produces a MAH yield of 20%, which is higher than that obtained with bulk zeolite catalyst under the same conditions (18%). It should be mentioned that the yield of water (not shown for the sake of clarity), produced by dehydration reactions from oxygenates, was 45% with bulk Z30, which is close to that produced with Cr-Z30 and Fe-Z30 (approximately 43%), and notably higher than that obtained with Zn-Z30 (24%). These results are consistent with the modification of acidity caused by each metal, as reported in the previous section.

It should be mentioned that during the catalytic cracking reaction, coke deposition occurs on the catalysts, leading to a decrease in the specific surface area. Table 2 compares the results of the coke content deposited, the BET specific surface area, and the percentage of surface loss (relative to the fresh values, Table 1) experienced by each catalyst during the process.

Table 2. Coke content (C_C), specific surface area (S_{BET}) and percentage of surface loss after reaction at 450 °C; 0.7 $g_{catal}h(g_{feed})^{-1}$ and 0.5 h time on stream.

	Bulk HZ-30	**Cr-Z30**	**Fe-Z30**	**Zn-Z30**
C_C (wt%)	12.8	12.1	10.8	10.1
S_{BET} (m^2 g^{-1})	93	87	105	107
Surface loss (%)	65	68	59	57

From the above catalyst screening, it can be concluded that doping with Fe_2O_3 promotes the production of monoaromatic hydrocarbons from bio-oil. Doping with Cr_2O_3, while slightly reducing the bio-oil conversion and hydrocarbon yield, is interesting due to its potential to increase the selectivity toward light olefins in the gaseous product. However, the addition of ZnO does not seem to be suitable for improving the performance of HZSM-5 zeolite in the production of hydrocarbons from bio-oil.

In order to evaluate the effect of the oxidation state of the metal species on hydrocarbon production, the behavior of the catalysts was studied after subjecting them to reduction prior to the catalytic cracking reaction. The reduction was conducted in situ (in the reactor), heating the fresh catalyst from room to 450 °C (rate of 10 °C min^{-1}) under 10 mL min^{-1} H_2/N_2 flow for 2 h.

The results using fresh Cr-Z30, Fe-Z30, and Zn-Z30 catalysts are compared with those obtained with reduced catalysts (Cr-Z30*, Fe-Z30*, and Zn-Z30*) in Figures 5, 6, and 7, respectively.

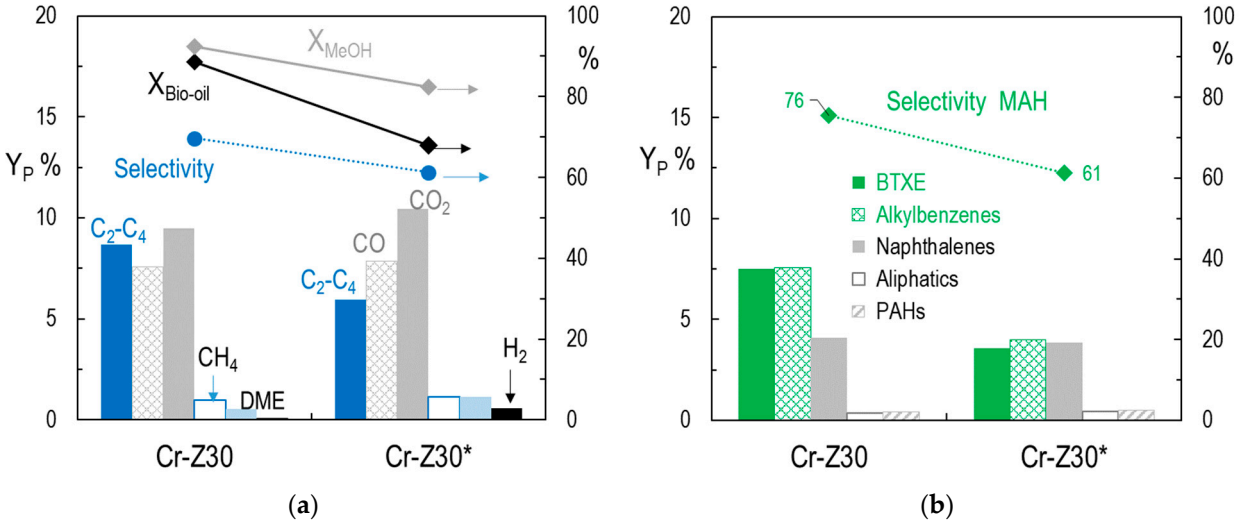

Figure 5. Comparison between fresh Cr-Z30 and reduced Cr-Z30* catalyst. (**a**) Feed conversion, gaseous product yields, and selectivity to light C_2–C_4 olefins; (**b**) liquid product yields and selectivity to monoaromatic hydrocarbons (MAH).

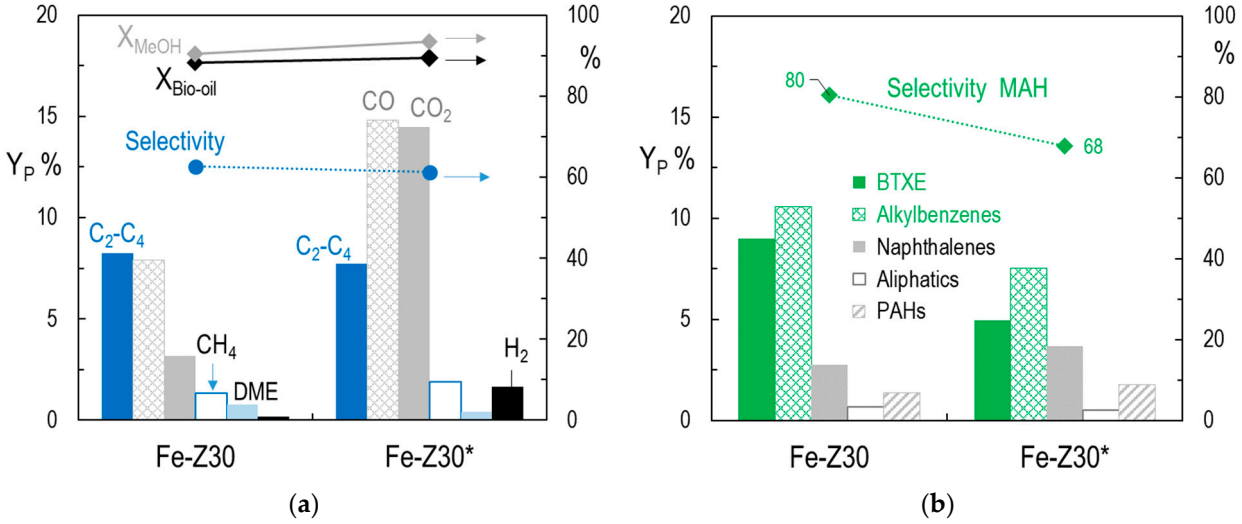

Figure 6. Comparison between fresh Fe-Z30 and reduced Fe-Z30* catalyst. (**a**) Feed conversion, gaseous product yields, and selectivity to light C_2–C_4 olefins; (**b**) liquid product yields and selectivity to monoaromatic hydrocarbons (MAH).

The results in Figure 5 show that, in the case of Cr-Z30, the prior in situ reduction has a negative effect on the catalyst behavior. There was a decrease of around 20% in bio-oil conversion and approximately 10% in methanol conversion (Figure 5a). Additionally, there is a negative effect on the yield of C_2–C_4 hydrocarbons (from 8.7% to 6%) and the selectivity to light C_2–C_4 olefins in the gaseous product, which decreases from 70% to 61%. It is worth noting that there is a slight increase in CO and CO_2 levels and the appearance of hydrogen in the gaseous product, with a yield of 0.6% (Figure 5a).

The results in Figure 5b also reveal that the reduced species of Cr in Cr-Z30* catalyst result in a lower yield of monoaromatics MAH (from 15% to 7.6%). The selectivity of MAH in liquid hydrocarbons is also negatively affected by the prior reduction, decreasing from values around 76% to 61%. The yield of the other hydrocarbons remains virtually unchanged.

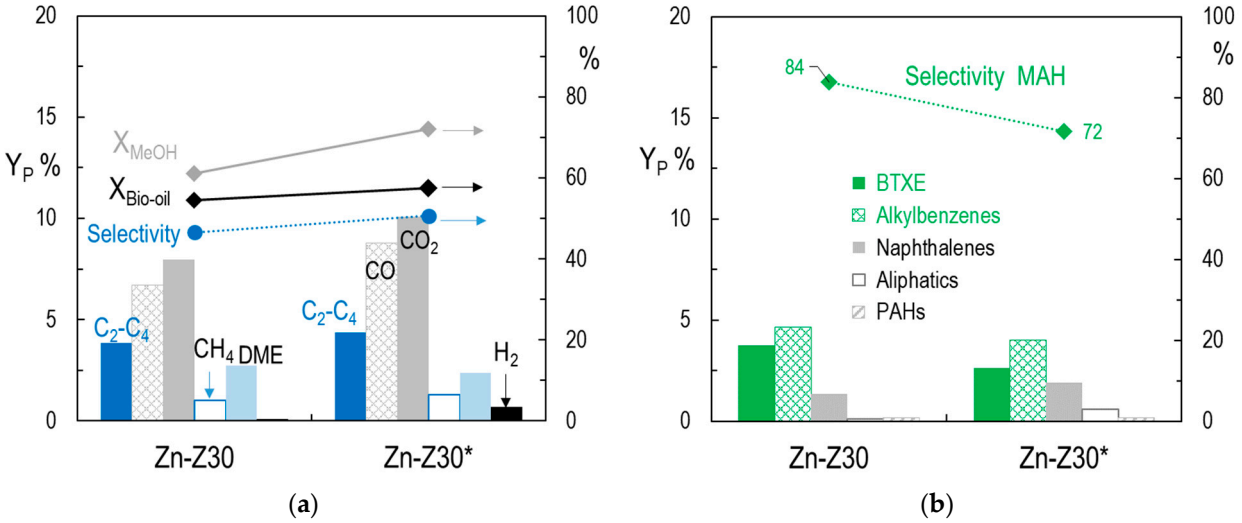

Figure 7. Comparison between fresh Zn-Z30 and reduced Zn-Z30* catalyst. (**a**) Feed conversion, gaseous product yields, and selectivity to light C_2–C_4 olefins; (**b**) liquid product yields and selectivity to monoaromatic hydrocarbons (MAH).

Conversely, in the case of Fe-Z30, the prior in situ reduction appears to have a slightly favorable effect on the conversion of oxygenates, increasing by 1% for bio-oil and by 3% for methanol (Figure 6a). However, the analysis of product yields reveals that the Fe species of in the reduced catalyst have lower activity for the production of hydrocarbons of interest. Thus, although the selectivity to light olefins is maintained around 62% (Figure 6a), the yield of light C_2–C_4 hydrocarbons slightly decreases with Fe-Z30* (from 8.2% to 7.7%). Notably, the yields of CO, and particularly that of CO_2, obtained with this catalyst are significant, and there is also a notable formation of H_2 in the gaseous product with a yield of 1.7% (Figure 6a).

The results in Figure 6b reveal that reduced Fe-Z30* catalyst produces a significantly lower yield of MAH (13%) compared with fresh Fe-Z30 catalyst (20%), while showing a slight increase in the yield of naphthalenes (from 2.7% to 3.7%) and polycyclic aromatic hydrocarbons PAHs (from 1.4% to 1.8%). The selectivity toward monoaromatic in liquid hydrocarbons decreases from 80% to 68%. This fact suggests that reduced Fe species activate dehydrogenation and condensation reactions, leading to heavier aromatics.

The results in Figure 7 show that, despite the Zn-Z30* catalyst still exhibiting poor activity, the prior in situ reduction has a slightly favorable effect on the conversion of oxygenates, especially for methanol, and in the production of light gaseous hydrocarbons. This leads to a slight increase in the C_2–C_4 yield, from 3.8% to 4.4%, and also an increase in selectivity toward C_2–C_4 olefins from 46% to 51% (Figure 7a). However, the yield and selectivity of MAH (Figure 7b) are negatively affected by the prior reduction, although with a less drastic effect compared to the previous catalysts.

For Cr-Z30 and Fe-Z30 catalysts, the yield of water produced during the reaction decreases when using the reduced catalysts, from approximately 44% to around 30%, while the reduction does not seem to affect the water yield in the case of Zn-Z30 catalyst, which remains at about 24%.

The results indicate that the reduced metal species primarily promote the formation of CO and CO_2, along with small amounts of H_2 in the gaseous product, at the expense of hydrocarbon formation. This suggests that decarbonylation reactions of oxygenates are preferentially activated, leading to CO formation, which may further produce CO_2 and H_2 through the water–gas–shift (WGS) reaction. This reaction is enhanced under the studied reaction conditions (450 °C and high water content in the reaction medium). The reduced Fe species also appear to activate hydrogen transfer reactions that promote condensation reactions, resulting in the formation of heavier aromatics.

3. Materials and Methods

3.1. Synthesis of Catalysts

The bulk HZSM-5 zeolite with SiO_2/Al_2O_3 ratio of 30 was provided by *Zeolyst International* (Conshohocken, PA, USA). The metal catalysts were prepared with a nominal metal content of 1 wt% by following an incipient wetness impregnation method using aqueous solutions of metal nitrates $Zn(NO_3)_2{\cdot}6H_2O$, $Cr(NO_3)_2{\cdot}9H_2O$, or $Fe(NO_3)_3{\cdot}9H_2O$. Each solution was added dropwise to the bulk zeolite at 60 ºC using a *BUCHI B-480* rotary evaporator (Buchi, Switzerland).

The bulk HZSM-5 and the metal containing zeolites were dried at 120 ºC overnight and then mixed with boehmite and α-Al_2O_3 in order to obtain a uniform slurry composed of 20 wt% α-Al_2O_3, 30 wt% boehmite, and 50 wt% zeolite [25]. The wet slurry was extruded and dried overnight at room temperature. The dried extrudates were then crushed, sieved in 150–300 µm size particles, and calcined for 5 h at 575 °C (heating rate of 5 °C min^{-1}) to obtain the final catalysts, which were denoted as Bulk Z30, Zn-Z30, Cr-Z30, and Fe-Z30.

It should be mentioned that agglomerating the zeolite within an alumina matrix improves the mechanical resistance of the catalyst for its use in a fluidized bed reactor and provides a mesoporous structure that enhance the diffusion and conversion of bulky bio-oil molecules [26–29].

3.2. Characterization of Catalysts

N_2-adsoption/desorption measurements were conducted on a *Micromeritics ASAP 2010* (MICROMERITICS, Norcross, GA, USA) for quantifying the textural properties. The specific surface area was determined by Brunauer–Emmet–Teller (BET) equation and the micropore volume was calculated using the t-plot method based on the Harkins–Jura equation. The mesopore volume was calculated as the difference between the total pore volume at P/P0 = 0.995 and the micropore volume.

The relative crystallinity of metal-doped catalysts was analyzed by a *Bruker D8 Advance X-ray* diffractometer (XRD) (BRUKER, Billerica, MA, USA). The metal loading on each catalyst was determined by X-ray fluorescence spectroscopy (XRF) using *PANalytical-AXIOS* spectrometer (Malvern Panalytical, Worcestershire, United Kingdom).

Temperature-programmed reduction analyses (TPR) were carried out on a *Micromeritics Autochem II 2920* (MICROMERITICS, Norcross, GA, USA) equipped with a thermal conductivity detector (TCD) by heating the sample from 50 to 800 °C in 10% H_2/N_2 flow. This equipment was also used to conduct NH_3 temperature-programmed desorption (NH_3-TPD) for determining the total acidity of the catalysts. In addition, the nature of the acid sites (Brønsted and Lewis) was explored by FTIR (Fourier transform infrared spectroscopy) of adsorbed pyridine on a *Nicolet 6700 FTIR* spectrometer (THERMO FISHER, Waltham, MA, USA).

3.3. Catalytic Cracking Experiments

The pyrolysis oil (bio-oil) originated from pine sawdust was provided by *BTG-Bioliquids* (Enschede, The Netherlands). The raw bio-oil was blended with methanol (Sigma-Aldrich, Burlington, MA, USA, ≥99.8%) serving as an effective stabilizer for storage purposes. The stabilized bio-oil, composed of 80 wt% raw bio-oil and 20 wt% methanol, possesses an enhanced H/C_{eff} ratio, which has proven advantageous for subsequent catalytic processes in terms of product selectivity and catalyst stability [30,31]. The stabilized bio-oil composition comprised 66 wt% of bio-oil-derived oxygenates, 16 wt% methanol, and 18 wt% water (quantified by Karl Fischer titration employing *KF Titrino Plus 870*, METROHM, Herisau, Switzerland). The detailed composition of bio-oil oxygenates was determined by gas chromatography/mass spectrometry conducted on *GC/MS Shimadzu QP2010* device (Shimadzu Corporation, Tokyo, Japan). Within this composition, the primary constituents identified were saccharides (19 wt%), phenols (17 wt%), esters (16 wt%), ketones (15 wt%), and acids (15 wt%).

The continuous two-step catalytic cracking system (TS-CC) employed for the catalytic cracking tests is depicted in Figure A1. This reaction equipment operates at atmospheric pressure conditions. The first thermal unit was employed to carefully deposit a carbonaceous solid (pyrolytic lignin), which is formed through re-polymerization of bio-oil oxygenates, predominantly phenolic compounds. The resulting volatile stream was subsequently directed into the in-line cracking unit (fluidized bed catalytic reactor). This configuration aimed to ensure controlled and efficient catalytic cracking processes, facilitating the transformation of the feedstock into desired products.

The volatile stream composition comprised 20 wt% water, 18 wt% methanol, and 62 wt% bio-oil oxygenates. Within these, the predominant compounds were esters (25 wt%), acids (23 wt%), ketones (18 wt%), saccharides (12 wt%), and phenols (7 wt%).

All the experiments were conducted at the same operating conditions: bio-oil feed flow-rate, 0.1 mL min^{-1}; thermal unit temperature, 500 °C; catalytic unit temperature, 450 °C; space-time 0.7 $g_{catalyst}$ $h(g_{feed})^{-1}$, time on stream, 0.5 h. The experiments with reduced catalysts were conducted after an in situ reduction with 10 mL min^{-1} H_2/N_2 flow for 2 h at 450 °C (heating rate of 10 °C min^{-1}).

3.4. Analysis of Reaction Products

During each experimental test, the gaseous product stream underwent in-line analysis using an *Agilent 490* micro-GC apparatus (AGILENT, Santa Clara, CA, USA) equipped with four distinct analytical modules. These modules facilitated quantification of the following compounds:

(1) H_2, N_2, CH_4, CO (MS5A column);
(2) C_4–C_{12} bio-oil oxygenates, C_{5+} hydrocarbons (CPSil 5CB column);
(3) CO_2, C_2–C_4 hydrocarbons, H_2O, MeOH, dimethyl ether, C_2–C_4 oxygenates (PPQ);
(4) C_6–C_{12} aromatics, C_6–C_{12} oxygenates (Stabilwax).

Subsequent to analysis, the product stream was cooled at the reactor outlet using a Peltier condenser. The resulting condensed mixture was collected within a steel vessel, allowing for further characterization. The detailed composition of C_{5+} hydrocarbons was analyzed by gas chromatography-mass spectrometry (*GC-MS Shimadzu QP2010* device, Shimadzu Corporation, Tokyo, Japan). These compounds were grouped according to their aliphatic and aromatic nature into BTXE (benzene, toluene, xylenes, ethylbenzene), gasoline-range C_5–C_{12} hydrocarbons (alkylbenzenes, naphthalenes, and aliphatics), and C_{12+} polyaromatics (PAHs).

3.5. Parameters for Quantifying the Catalytic Behavior

The performance of bulk zeolite catalyst and catalysts doped with metals was assessed concerning the conversion of reactants (bio-oil oxygenates and methanol present in the feed), yields of products, and selectivity to specific hydrocarbons. Of particular interest was the production of light C_2–C_4 olefins and monoaromatics (including BTXE and alkylbenzenes).

The resulting products from the reaction were categorized into two groups: hydrocarbons (CH_4, C_2–C_4, C_{5+}) and deoxygenation products (CO, CO_2, H_2O). The determination of conversion and product yields was based on the mass flow rate of each lump (or compound) at both the inlet and outlet of the catalytic reactor, in accordance with the subsequent equations:

$$X_i = \frac{F_i^{in} - F_i^{out}}{F_i^{in}} \cdot 100 \quad (1)$$

$$Y_P = \frac{F_P^{out}}{F_{bio-oil}^{in} + F_{MeOH}^{in}} \cdot 100 \quad (2)$$

where F_i^{in} is the mass flow-rate (g min^{-1}) of oxygenates (i = bio-oil and methanol) at the inlet, F_i^{out} is the mass flow-rate (g min^{-1}) of oxygenates at the outlet of the reactor, and F_P^{out} is the mass flow-rate of product (p = C_{5+}, C_2–C_4, CH_4, CO+CO_2, H_2O). The individual

yield of each component within the C_{5+} hydrocarbons (BTEX, alkylbenzenes, naphthalenes, aliphatics, and PAHs) was determined from the total yield (Y_{C5+}) and the content of each lump present. This content was obtained from the GC-MS analysis of the collected organic fraction.

The selectivity to C_2–C_4 olefins (C_2–$C_4^=$) and monoaromatic hydrocarbons (MAH) was quantified from product yields according to Equation (3) and Equation (4), respectively.

$$\text{Selectivity } C_2\text{–}C_4^= = \frac{Y_{C_2\text{–}C_4^=}}{Y_{C2\text{–}C4}} \cdot 100 \quad (3)$$

$$\text{Selectivity MAH} = \frac{Y_{MAH}}{Y_{C5+}} \cdot 100 \quad (4)$$

4. Conclusions

This study focuses on the comparative evaluation of transition metal doped HZSM-5 catalysts for the catalytic cracking of raw bio-oil. The findings contribute to a better understanding of the impact that the metal species have on the zeolite activity for the conversion of oxygenates and selectivity toward hydrocarbon products.

The addition of chromium, iron, and zinc influences the catalytic behavior of HZSM-5, affecting its activity and selectivity. The zinc-doped zeolite (Zn-Z30) exhibits poor activity with significantly lower bio-oil conversion compared to the bulk zeolite (Bulk Z30). On the other hand, chromium and iron-doped zeolites (Cr-Z30 and Fe-Z30) show slightly lower conversion but maintain relatively high activity.

In general, the yields of light C_2–C_4 hydrocarbons decrease with metal-doped catalysts compared to the bulk zeolite, while the selectivity toward light olefins slightly increases. The incorporation of Fe promotes the production of monoaromatic hydrocarbons, whereas Cr shows potential to increase the selectivity toward light olefins. However, Zn doping do not enhance the performance of HZSM-5 zeolite in hydrocarbon production from bio-oil.

The oxidation state of the metal species plays a significant role in catalytic activity, with reduced metal species primarily promoting the formation of CO and CO_2, along with low amounts of H_2, at the expense of hydrocarbon formation. Decarbonylation reactions of oxygenates leading to CO formation seem preferentially activated, and the water–gas–shift (WGS) reaction plays a role in producing CO_2 and H_2. The reduced Fe species also activate hydrogen transfer reactions, promoting the formation of heavier aromatics.

Based on the findings of this study, careful consideration should be given to the selection of metal species to achieve the desired performance of HZSM-5 zeolite for the catalytic cracking of feedstock with complex composition such is the raw bio-oil.

In conclusion, this study provides valuable insights into the catalytic cracking of bio-oil using metal-doped HZSM-5 catalysts. The findings have direct applicability to the scaling-up of bio-oil valorization process and can guide the design of highly active and selective catalysts for bio-oil upgrading.

Author Contributions: M.E.C.: investigation, formal analysis, visualization; I.C.: investigation, formal analysis; A.B.M.: supervision, writing—original draft preparation; B.V.: conceptualization, funding acquisition, supervision, writing—original draft preparation, writing—review and editing, project administration. All authors have read and agreed to the published version of the manuscript.

Funding: This research was funded by the Ministry of Science and Innovation of the Spanish Government (grant number RTI2018-095990-J-I00 funded by MCIN/AEI/10.13039/501100011033 and by "ERDF A way of making Europe"); Department of Education, Universities and Investigation of the Basque Government (Project IT1645-22); University of the Basque Country (grant UPV/EHU PIF 2021 of Iratxe Crespo).

Data Availability Statement: Not applicable.

Acknowledgments: The authors thank for technical and human support provided by SGIker (UPV/EHU/ERDF, EU).

Conflicts of Interest: The authors declare no conflict of interest.

Appendix A

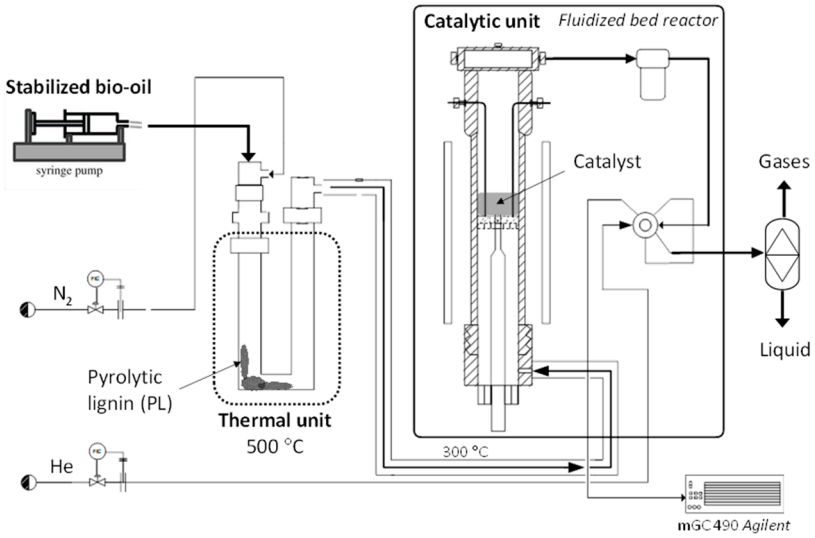

Figure A1. Schematic diagram of the continuous two-step catalytic cracking system (TS-CC).

References

1. Hansen, S.; Mirkouei, A.; Diaz, L.A. A Comprehensive State-of-Technology Review for Upgrading Bio-Oil to Renewable or Blended Hydrocarbon Fuels. *Renew. Sustain. Energy Rev.* **2020**, *118*, 109548. [CrossRef]
2. Valle, B.; Remiro, A.; García-Gómez, N.; Gayubo, A.G.; Bilbao, J. Recent Research Progress on Bio-Oil Conversion into Bio-Fuels and Raw Chemicals: A Review. *J. Chem. Technol. Biotechnol.* **2019**, *94*, 670–689. [CrossRef]
3. Liang, J.; Shan, G.; Sun, Y. Catalytic Fast Pyrolysis of Lignocellulosic Biomass: Critical Role of Zeolite Catalysts. *Renew. Sustain. Energy Rev.* **2021**, *139*, 110707. [CrossRef]
4. Puértolas, B.; Veses, A.; Callén, M.S.; Mitchell, S.; García, T.; Pérez-Ramírez, J. Porosity–Acidity Interplay in Hierarchical ZSM-5 Zeolites for Pyrolysis Oil Valorization to Aromatics. *ChemSusChem* **2015**, *8*, 3283–3293. [CrossRef] [PubMed]
5. Cai, Q.; Yu, T.; Meng, X.; Zhang, S. Selective Generation of Aromatic Hydrocarbons from Hydrotreating-Cracking of Bio-Oil Light Fraction with MO_x Modified HZSM-5 (M = Ga, Mo and Zn). *Fuel Process. Technol.* **2020**, *204*, 106424. [CrossRef]
6. Zheng, Y.; Wang, F.; Yang, X.; Huang, Y.; Liu, C.; Zheng, Z.; Gu, J. Study on Aromatics Production via the Catalytic Pyrolysis Vapor Upgrading of Biomass Using Metal-Loaded Modified H-ZSM-5. *J. Anal. Appl. Pyrolysis* **2017**, *126*, 169–179. [CrossRef]
7. Chaihad, N.; Karnjanakom, S.; Abudula, A.; Guan, G. Zeolite-Based Cracking Catalysts for Bio-Oil Upgrading: A Critical Review. *Resour. Chem. Mater.* **2022**, *1*, 167–183. [CrossRef]
8. Kosinov, N.; Liu, C.; Hensen, E.J.M.; Pidko, E.A. Engineering of Transition Metal Catalysts Confined in Zeolites. *Chem. Mater.* **2018**, *30*, 3177–3198. [CrossRef]
9. Valle, B.; Gayubo, A.G.; Aguayo, A.T.; Olazar, M.; Bilbao, J. Selective Production of Aromatics by Crude Bio-Oil Valorization with a Nickel-Modified HZSM-5 Zeolite Catalyst. *Energy Fuels* **2010**, *24*, 2060–2070. [CrossRef]
10. Iliopoulou, E.F.; Stefanidis, S.D.; Kalogiannis, K.G.; Delimitis, A.; Lappas, A.A.; Triantafyllidis, K.S. Catalytic Upgrading of Biomass Pyrolysis Vapors Using Transition Metal-Modified ZSM-5 Zeolite. *Appl. Catal. B Environ.* **2012**, *127*, 281–290. [CrossRef]
11. Argyle, D.M.; Bartholomew, H.C. Heterogeneous Catalyst Deactivation and Regeneration: A Review. *Catalysts* **2015**, *5*, 145–269. [CrossRef]
12. Razzaq, M.; Zeeshan, M.; Qaisar, S.; Iftikhar, H.; Muneer, B. Investigating Use of Metal-Modified HZSM-5 Catalyst to Upgrade Liquid Yield in Co-Pyrolysis of Wheat Straw and Polystyrene. *Fuel* **2019**, *257*, 116119. [CrossRef]
13. Sun, L.; Zhang, X.; Chen, L.; Zhao, B.; Yang, S.; Xie, X. Effects of Fe Contents on Fast Pyrolysis of Biomass with Fe/CaO Catalysts. *J. Anal. Appl. Pyrolysis* **2016**, *119*, 133–138. [CrossRef]
14. Mohiuddin, E.; Mdleleni, M.M.; Key, D. Catalytic Cracking of Naphtha: The Effect of Fe and Cr Impregnated ZSM-5 on Olefin Selectivity. *Appl. Petrochem. Res.* **2018**, *8*, 119–129. [CrossRef]
15. Che, Q.; Yang, M.; Wang, X.; Yang, Q.; Rose Williams, L.; Yang, H.; Zou, J.; Zeng, K.; Zhu, Y.; Chen, Y.; et al. Influence of Physicochemical Properties of Metal Modified ZSM-5 Catalyst on Benzene, Toluene and Xylene Production from Biomass Catalytic Pyrolysis. *Bioresour. Technol.* **2019**, *278*, 248–254. [CrossRef]
16. Wang, D.; Jin, L.; Li, Y.; Wei, B.; Yao, D.; Hu, H. Effect of Reducibility of Transition Metal Oxides on In-Situ Oxidative Catalytic Cracking of Tar. *Energy Convers. Manag.* **2019**, *197*, 111871. [CrossRef]

17. Emeis, C.A. Determination of Integrated Molar Extinction Coefficients for Infrared Absorption Bands of Pyridine Adsorbed on Solid Acid Catalysts. *J. Catal.* **1993**, *141*, 347–354. [CrossRef]
18. Chen, H.-Y.; Sachtler, W.M.H. Activity and Durability of Fe/ZSM-5 Catalysts for Lean Burn NOx Reduction in the Presence of Water Vapor. *Catal. Today* **1998**, *42*, 73–83. [CrossRef]
19. Denardin, F.; Perez-Lopez, O.W. Tuning the Acidity and Reducibility of Fe/ZSM-5 Catalysts for Methane Dehydroaromatization. *Fuel* **2019**, *236*, 1293–1300. [CrossRef]
20. Jiménez-López, A.; Rodríguez-Castellón, E.; Maireles-Torres, P.; Díaz, L.; Mérida-Robles, J. Chromium Oxide Supported on Zirconium- and Lanthanum-Doped Mesoporous Silica for Oxidative Dehydrogenation of Propane. *Appl. Catal. A Gen.* **2001**, *218*, 295–306. [CrossRef]
21. Karami, H.; Soltanali, S.; Najafi, A.M.; Ghazimoradi, M.; Yaghoobpour, E.; Abbasi, A. Amorphous Silica-Alumina as Robust Support for Catalytic Dehydrogenation of Propane: Effect of Si/Al Ratio on Nature and Dispersion of Cr Active Sites. *Appl. Catal. A Gen.* **2023**, *658*, 119167. [CrossRef]
22. Wan, B.-Z.; Chu, H.M. Reaction Kinetics of Propane Dehydrogenation over Partially Reduced Zinc Oxide Supported on Silicalite. *J. Chem. Soc. Faraday Trans.* **1992**, *88*, 2943–2947. [CrossRef]
23. Lai, S.; She, Y.; Zhan, W.; Guo, Y.; Guo, Y.; Wang, L.; Lu, G. Performance of Fe-ZSM-5 for Selective Catalytic Reduction of NO_x with NH3: Effect of the Atmosphere during the Preparation of Catalysts. *J. Mol. Catal. A Chem.* **2016**, *424*, 232–240. [CrossRef]
24. de Oliveira, T.K.R.; Rosset, M.; Perez-Lopez, O.W. Ethanol Dehydration to Diethyl Ether over Cu-Fe/ZSM-5 Catalysts. *Catal. Commun.* **2018**, *104*, 32–36. [CrossRef]
25. Pérez-Uriarte, P.; Gamero, M.; Ateka, A.; Díaz, M.; Aguayo, A.T.; Bilbao, J. Effect of the Acidity of HZSM-5 Zeolite and the Binder in the DME Transformation to Olefins. *Ind. Eng. Chem. Res.* **2016**, *55*, 1513–1521. [CrossRef]
26. Bertero, M.; García, J.R.; Falco, M.; Sedran, U. Hydrocarbons from Bio-Oils: Performance of the Matrix in FCC Catalysts in the Immediate Catalytic Upgrading of Different Raw Bio-Oils. *Waste Biomass Valorization* **2017**, *8*, 933–948. [CrossRef]
27. Crespo, I.; Hertzog, J.; Carré, V.; Aubriet, F.; Valle, B. Alumina-Embedded HZSM-5 with Enhanced Behavior for the Catalytic Cracking of Biomass Pyrolysis Bio-Oil: Insights into the Role of Mesoporous Matrix in the Deactivation by Coke. *J. Anal. Appl. Pyrolysis* **2023**, *172*, 106009. [CrossRef]
28. Arumugam, M.; Goh, C.K.; Zainal, Z.; Triwahyono, S.; Lee, A.F.; Wilson, K.; Taufiq-Yap, Y.H. Hierarchical HZSM-5 for Catalytic Cracking of Oleic Acid to Biofuels. *Nanomaterials* **2021**, *11*, 747. [CrossRef]
29. Gao, J.; Zhou, H.; Zhang, F.; Ji, K.; Liu, P.; Liu, Z.; Zhang, K. Effect of Preparation Method on the Catalytic Performance of HZSM-5 Zeolite Catalysts in the MTH Reaction. *Materials* **2022**, *15*, 2206. [CrossRef]
30. Gayubo, A.G.; Valle, B.; Aguayo, A.T.; Olazar, M.; Bilbao, J. Attenuation of Catalyst Deactivation by Cofeeding Methanol for Enhancing the Valorisation of Crude Bio-Oil. *Energy Fuels* **2009**, *23*, 4129–4136. [CrossRef]
31. Du, L.; Luo, Z.; Wang, K.; Miao, F.; Qian, Q. Catalytic Co-Conversion of Poplar Pyrolysis Vapor and Methanol for Aromatics Production via Ex-Situ Configuration. *J. Anal. Appl. Pyrolysis* **2022**, *165*, 105571. [CrossRef]